Chin. Phys. B Vol. 21, No. 12 (2012) 128504

Improved efficiency droop characteristics in InGaN/GaN light-emitting diode with a novel designed last barrier structure*

Wang Tian-Hu(王天虎) and Xu Jin-Liang (徐进良)†

Beijing Key Laboratory of New and Renewable Energy, North China Electric Power University, Beijing 102206*, China*

(Received 10 May 2012; revised manuscript received 10 June 2012)

In this study, the characteristics of the nitride-based light-emitting diodes with different last barrier structures are analysed numerically. The energy band diagrams, electrostatic field near the last quantum barrier, carrier concentration in the quantum well, internal quantum efficiency, and light output power are systematically investigated. The simulation results show that the efficiency droop is markedly improved and the output power is greatly enhanced when the conventional GaN last barrier is replaced by AlGaN barrier with Al composition graded linearly from 0 to 15% in the growth direction. These improvements are attributed to enhanced efficiencies of electron confinement and hole injection caused by the less polarization effect at the last-barrier/electron blocking layer interface when the graded Al composition last barrier is used.

Keywords: light-emitting diodes, internal quantum efficiency, efficiency droop, last barrier

PACS: 85.60.Jb, 85.50.–n, 87.15.A–, 78.60.Fi **DOI:** 10.1088/1674-1056/21/12/128504

1. Introduction

III-nitride light-emitting diodes (LEDs) have many applications such as in full colour displays, back lighting, and general illumination.[1–5] However, the InGaN LEDs suffer from the problem of efficiency droop at high current.[3] Thus, this phenomenon leads to great restriction on the development of high power solid state lighting. Over the past few years, several reasons accounting for the existence of efficiency droop have been suggested.[2,3,6–13] However, the origin mechanism remains controversial untill now. Among these factors, the insufficient electron confinement and poor hole injection efficiency are considered to play a key role in this issue. In the InGaN/GaN multi-quantum well (MQW) LED, the strong piezoelectric polarization field is generated due to the fact that the lattice mismatch between GaN barrier and AlGaN electron blocking layer (EBL) will pull down the conduction band at the last-barrier/EBL interface.[2,7,14] The band bending lowers the effective barrier height of the AlGaN EBL significantly, which is inconducive to the confinement of electrons. On the other hand, the hole injection is also reduced seriously due to the band bending caused by the polarization effect.[6,12,14] Consequently, electron leakage together with poor hole injection leads to the reduced internal quantum efficiency (IQE).

To solve the above problems, many droop improvement strategies are employed to enhance the capability of electron confinement[2,4,6–8,12,13] and to increase the hole injection efficiency.[9–13] These methods have resulted in marked improvement in efficiency droop for LEDs. Besides, Chen *et al.*[15] reported that the using of a p-type GaN last barrier before the growth of AlGaN EBL can provide a higher energy barrier to suppress the electron overflow and then enhance the light output power. The effects of last barrier thickness on the device performance are discussed in the work. Yen *et al.*'s investigation[16] indicates that the radiative recombination and optical power are enhanced when a thin last barrier is utilized. A partially p-doped last barrier to overcome the aforementioned restrictions and thus to improve the IQE is also proposed.[17] It is believed that the last barrier plays a significant role in the effects of electron leakage and hole injection efficiency. However, in Refs. [15]–[17], the last barriers are all of the conventional design of GaN, which leads to large po-

---

*Project supported by the National Natural Science Foundation of China (Grant Nos. U1034004 and 50825603) and the Fundamental Research Funds for the Central Universities, China (Grant Nos. 12QX14 and 11ZG01).

†Corresponding author. E-mail: xjl@ncepu.edu.cn

larization at the last-barrier/EBL interface. In this paper, we design a novel Al composition graded last barrier (GLB) for InGaN/GaN LED employing the concept of band-engineering.

The concept of GLB was obtained from the observation on the band diagram near the last barrier and EBL. For the conventional GaN last barrier, there is a strong piezoelectric polarization field at the last-barrier/EBL interface due to the lattice mismatch between GaN barrier and AlGaN EBL, and it will reduce the IQE. However, theoretically, if the conventional GaN last barrier is replaced by $Al_xGa_{1-x}N$ barrier with Al composition graded linearly in the growth direction, the influence of polarization-induced downward bending at the interface should be mitigated due to higher-quality lattice-match. Consequently, improved effective height of the EBL can be obtained, which can enhance the efficiency of electron confinement and hole injection, thus the IQE will be improved. To prove the above hypothesis, three LED structures with different last barriers are investigated by APSYS program. The GLB used in this paper not only suppresses the electron overflow out of the active region but also enhances the hole injection due to the less polarization effect at the last-barrier/EBL interface.

2. LED structures and physical parameters

The original LED structure used as a reference was prepared on a *c*-plane sapphire substrate. Before the growth of InGaN/GaN multi-quantum wells, a 50-nm-thick un-doped GaN buffer layer was deposited and then a 3-μm-thick Si-doped n-type GaN layer was grown (n-doping=5×10^{18} cm^{-3}). The active region consists of five 4-nm-thick $In_{0.08}Ga_{0.92}N$ quantum wells, separated by six 10-nm-thick GaN barriers. On the top of the active region were a 20-nm-thick p-type $Al_{0.15}Ga_{0.85}N$ EBL (p-doping $=1\times10^{18}$ cm^{-3}) and a 0.25-μm-thick p-type GaN cap layer (p-doping $=1.2\times10^{18}$ cm^{-3}). The device geometry was 200 μm×300 μm. Figure 1 shows the schematic diagram of the original and novel designed structures. Structure A denotes the original LED, the new designed structures B and C are the same as the original LED except that the last GaN barrier (the barrier nearest to the EBL which is shown in Fig. 1) is replaced by the $Al_xGa_{1-x}N$ barriers with the linearly graded Al composition x varied from 0 to 0.10 (structure B) and 0.15 (structure C) in the growth direction, respectively.

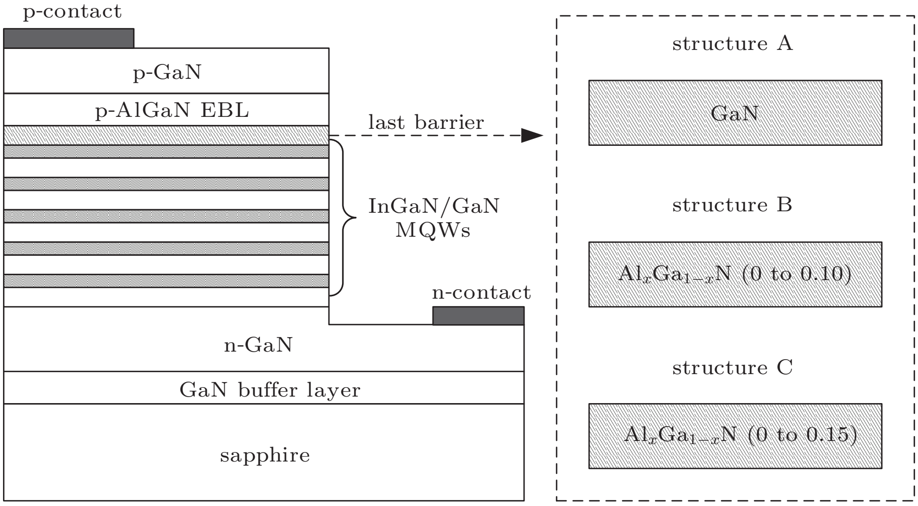

Fig. 1. Schematic diagram of the original structure (structure A), structure B, and structure C. The last barriers of the three LEDs are all plotted on the right-hand side of the figure.

The optical and electrical properties of the LEDs were investigated numerically with the APSYS simulation program, which is developed by the Crosslight Software Inc.[18] APSYS software is capable of dealing with the physical properties of LEDs by solving the Poisson's equation, current continuity equations, carrier transport equation, quantum mechanical wave equation, photon rate equation, and heat transfer equations. Because the above equations are coupled and nonlinear, there is no method to solve the equations in one direct step. Instead, solutions must be obtained by a nonlinear iteration method. The equations are discretized by the finite element method, and the Newton–Raphson method is used to solve the above equations. Besides, because an LED chip has different regions and its electrical and optical parameters are different from region to region, the non-uniform grids were used here. Fine grids were allocated in the n-GaN, EBL, and p-GaN regions. Very fine grids were used in the active region, specially. Coarse grids were used in the substrate. The grid independence was carefully examined during the preliminary test runs. APSYS employs the 6×6 $k\cdot p$ model, which is developed by Chuang and Chang,[19,20] to calculate the energy band structures. The method developed by Fiorentini *et al.*[21] was employed to estimate the built-in polarization caused by the spontaneous and piezoelectric polarization at the hetero-interfaces of III-nitride semiconductor device. Considering the screening caused by defects, the surface charge densities are assumed to be 50% of the calculated values. The internal absorption within the LED device and the light extraction efficiency are assumed to be $2000\ \mathrm{m}^{-1}$ and 78%, respectively. The Shockley–Read–Hall (SRH) recombination lifetime is set to be 100 ns. Other material parameters of the semiconductors used in the simulation can be found in Ref. [22].

3. Results and discussion

Figure 2 shows the energy band diagrams and quasi-Fermi levels of the three LED structures at 180 mA. Figure 2(a) shows that there is a serious tilting of energy band at the last-barrier/EBL interface with conventional GaN last barrier due to relatively strong polarization field. As indicated in Fig. 2(b), the use of GLB ($x = 0.10$) is beneficial to enhancing the effective height of the EBL for electron confinement (i.e., 437 meV versus 408 meV), hence, more electrons can stay in the QWs and recombine with holes. When the electrons overflowing to the p-layers are diminished, the efficiency of hole injection into the active region can be enhanced because there are fewer holes that would recombine with leaked electrons before they are injected into the active region. Besides, the effective potential height for holes in the valence band of structure B is lower than that of structure A (i.e. 433 meV versus 458 meV), owing to the slighter polarization effect in the last-barrier/EBL interface, which leads to better hole injection efficiency. Moreover, as shown in Fig. 2(c), the effective barrier height for electron confinement in the conduction band increases from 408 meV to 458 meV, and the potential in the valence band decreases significantly from 458 meV to 417 meV as compared with those in the original structure. Consequently, the capability of electrons confinement is effectively improved and the hole injection efficiency is markedly enhanced when the last GaN barrier is replaced by GLB ($x = 0.15$).

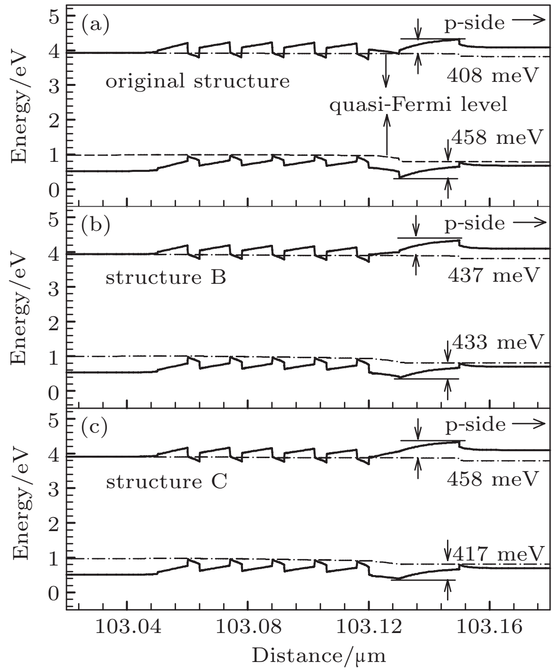

Fig. 2. Energy band diagrams for (a) original structure, (b) structure B, and (c) structure C at injection current of 180 mA.

These phenomena can be verified by the electrostatic fields near the last two QWs and EBL at 180 mA which are plotted in Fig. 3. Evidently, the original structure possesses the strongest electrostatic field in the last-barrier/EBL interface because of the severe lattice mismatch between the last GaN barrier and the AlGaN EBL, which leads to the situation of band bending (see Fig. 2(a)), poor overlap of electron, and hole wave functions, and hence reduced radiative recombination rate (see Fig. 6). Due to higher-quality lattice-match obtained by replacing the last GaN barrier with GLB ($x = 0.10$) in structure B, the surface charge density decreases and thus the electrostatic field is alleviated (i.e. -0.079 MV/cm versus -0.249 MV/cm). It can significantly lower the degree of polarization-induced band bending by using the GLB ($x = 0.10$). Moreover, the electrostatic field in the last-barrier/EBL interface is almost unobservable in structure C, which is much smaller than those in structure A (i.e. 0.010 MV/cm versus −0.249 MV/cm) and structure B (i.e. 0.010 MV/cm versus −0.079 MV/cm). Therefore, the downward band-bending at the last-barrier/EBL interface of structure C is the slightest in the three LED structures, which will increase the effective height of conduction band and reduce the barrier potential of the valence band for the EBL, leading to the enhanced efficiency of electron confinement and hole injection. As observed in Fig. 3, the electrostatic fields in quantum wells for structure C are also much less than those for structures A and B. Specifically, the amplitude of the electrostatic field in the last quantum well decreases from −0.376 MV/cm to −0.326 MV/cm as compared with that of the original structure. Therefore, the overlap of electron and hole wave functions, and the radiative recombination rate are strongest in structure C (see Fig. 6). As a result, it is predicted that structures B and C will provide more effective confinement for electrons from overflowing to the p-type layer and higher hole injection efficiency, which thus results in less severe electron leakage (see Fig. 4).

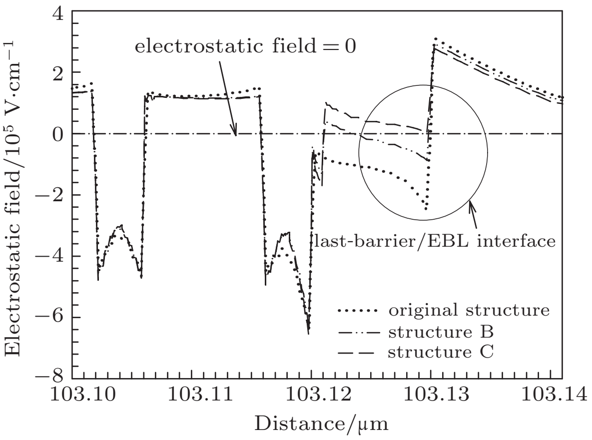

Fig. 3. Electrostatic fields near the last two QWs and EBLs of the three LEDs at 180 mA.

Figure 4 shows the electron current leakage ratios of the three LEDs. The electron current leakage ratio is defined as the ratio between the current leakage which overflows from the active region to the p-type layer and the injection current ($\delta = I_{\rm leak}/I_{\rm in}$). As shown in Fig. 4, there are fewer electrons contributing to the recombination in the QWs, which results in severe leakage current in the original structure. In structures B and C, with using the proposed last barriers, the electron leakage current is significantly suppressed. δ of structure B is greatly less than that of the original structure at the same injection current. The difference in δ between the original structure and structure C becomes larger with injection current increasing, which is of benefit to the confinement of electrons at high current. Moreover, the values of δ for the three structures increase with injection current increasing. Thus, the electron current leakage may play an important role in the efficiency droop and optical properties of InGaN LEDs.

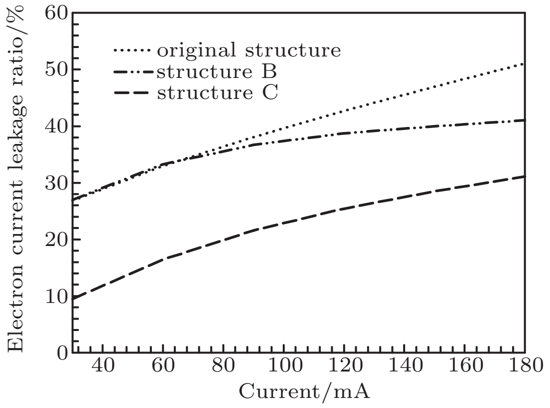

Fig. 4. Electron leakage ratios versus injection current for the original structure, structure B, and structure C.

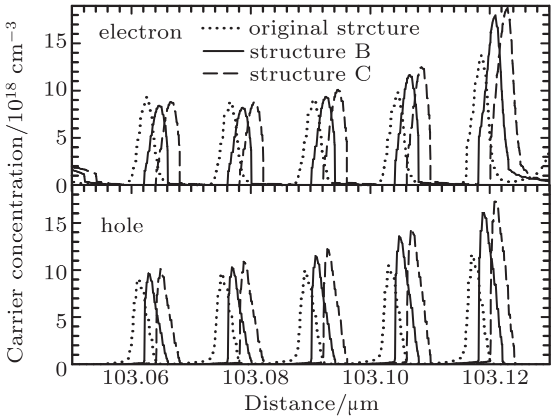

Fig. 5. Carrier concentrations within the active regions for the original structure, structure B, and structure C at an injection current of 180 mA.

Figure 5 shows the electron and hole concentrations within the active regions of the three LEDs at 180 mA. Note that the horizontal positions of the GLB LEDs have been shifted slightly for better observation. Both the electron and hole concentrations of structures B and C are higher than those of the original one, which demonstrates the improved capability of electron confinement and enhanced hole injection efficiency. Figure 6 shows the radiative recombination rates of the three LEDs around the active regions at 180 mA. Obviously, when the conventional last barrier is replaced by GLBs, the QWs can make more contributions to radiative recombination, owing to the remarkable improvement on electron and hole concentration inside the active region. Compared with the original structure, structure B and structure C have the total radiative recombination rates that are enhanced by factors of 5.97% and 24.71%, respectively. Thus, the internal quantum efficiency of the LED structure can be improved when the last barrier is replaced by GLB ($x = 0.15$) due to slighter polarization mismatch at the last-barrier/EBL interface.

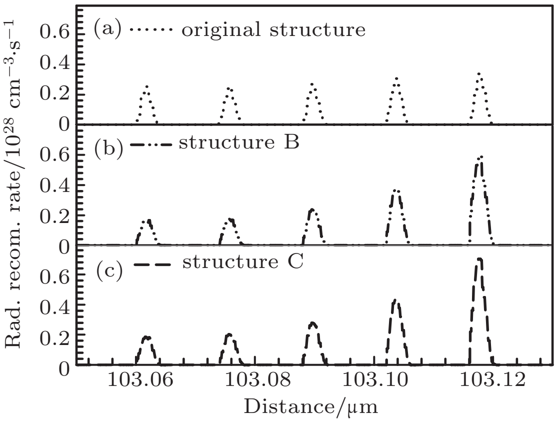

Fig. 6. Radiative recombination rates for (a) original structure, (b) structure B, and (c) structure C at an injection current of 180 mA.

Figure 7 shows the curves of simulated IQE and output power versus injection current for conventional and GLB LEDs. It is indicated that the GLB ($x = 0.15$) structure has the highest IQE and light output power at 180 mA. If the droop ratio η is defined as $\eta = (IQE_{\max} - IQE_{\min})/IQE_{\max}$, the conventional LED exhibits a serious efficiency droop with a droop ratio of 36.0%. The efficiency droop ratio decreases from 36.0% of the original structure to 27.9% of the structure B, and to 24.7% of the structure C. The enhancement of IQE leads to the improvement on output power. The ratios of improved output power for structures B and C are 1.21 and 1.41 at 180 mA, respectively compared with that for the original structure. The GLB ($x = 0.15$) LED is the best choice for high-power application in the three LED structures due to its smallest efficiency droop.

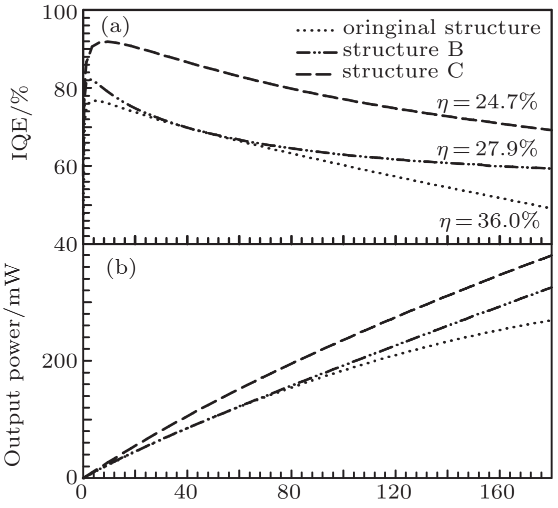

Fig. 7. Curves of (a) internal quantum efficiency and (b) light output power versus injection current for the three LED structures.

4. Conclusions

In this paper, InGaN/GaN MQWs LEDs with the conventional and graded last barriers are investigated numerically. When the last GaN barrier is replaced by an AlGaN GLB, the influence of polarization-induced downward bending in the last-barrier/EBL interface is mitigated due to higher-quality lattice-match. Consequently, improved effective height of the EBL can be obtained, which enhances the electron confinement and makes more holes transport from the p-type region into the active region. This effect prevents the electron leakage and improves the radiative recombination rate in the quantum well, leading to significant improvement on light output power and IQE.

References

[1] Krames M R, Shchekin O B, Mueller-Mach R, Müller G O, Zhou L, Harbers G and Craford M G 2007 *IEEE J. Disp. Technol.* **3** 160

[2] Kim M H, Schubert M F, Dai Q, Kim J K, Schubert E F, Piprek J and Park Y 2007 *Appl. Phys. Lett.* **91** 183507

[3] Gardner N F, Müller G O, Shen Y C, Chen G, Watanabe S, Götz W and Krames M R 2007 *Appl. Phys. Lett.* **91** 243506

[4] Lu T P, Li S T, Zhang K, Liu C, Xiao G W, Zhou Y G, Zheng S W, Yin Y A, Wu L J, Wang H L and Yang X D 2011 *Chin. Phys.* B **20** 108504

[5] Gong C C, Fan G H, Zhang Y Y, Xu Y Q, Liu X P, Zheng S W, Yao G R and Zhou D T 2012 *Chin. Phys.* B **21** 068505

[6] Schubert M F, Xu J, Kim J K, Schubert E F, Kim M H, Yoon S, Lee S M, Sone C, Sakong T and Park Y 2008 *Appl. Phys. Lett.* **93** 041102

[7] Zhang Y Y and Fan G H 2011 *Chin. Phys.* B **20** 048502

[8] Lu T P, Li S T, Zhang K, Liu C, Xiao G W, Zhou Y G, Zheng S W, Yin Y A, Wu L J, Wang H L and Yang X D 2011 *Chin. Phys.* B **20** 098503

[9] Rozhansky I V and Zakheim D A 2007 *Phys. Status Solidi* A **204** 227

[10] Xie J, Ni X, Fan Q, Shimada R, Özgür Ü and Morkoc H 2008 *Appl. Phys. Lett.* **93** 121107

[11] Ni X, Fan Q, Shimada R, Özgür Ü and Morkoc H 2008 *Appl. Phys. Lett.* **93** 171113

[12] Wang C H, Ke C C, Lee C Y, Chang S P, Chang W T, Li J C, Li Z Y, Yang H C, Kuo H C, Lu T C and Wang S C 2010 *Appl. Phys. Lett.* **97** 261103

[13] Wu L J, Li S T, Liu C, Wang H L, Lu T P, Zhang K, Xiao G W, Zhou Y G, Zheng S W, Yin Y A and Yang X D 2012 *Chin. Phys.* B **21** 068506

[14] Chen J, Fan G H, Zhang Y Y, Pang W, Zheng S W and Yao G R 2012 *Chin. Phys.* B **21** 058504

[15] Chen J R, Lu T C, Kuo H C, Fang K L, Huang K F, Kuo C W, Chang C J, Kuo C T and Wang S C 2010 *IEEE Photon. Technol. Lett.* **22** 860

[16] Yen S H, Tsai M L, Tsai M C, Chang S J and Kuo Y K 2010 *IEEE Photon. Technol. Lett.* **22** 1787

[17] Kuo Y K, Tsai M C, Yen S H, Hsu T C and Shen Y J 2010 *IEEE J. Quantum Electron* **46** 1214

[18] APSYS by Crosslight Software Inc., Burnaby, Canada (http://www.crosslight.com)

[19] Chuang S L and Chang C S 1996 *Phys. Rev.* B **54** 2491

[20] Chuang S L and Chang C S 1997 *Semicond. Sci. Technol.* **12** 252

[21] Fiorentini V, Bernardini F and Ambacher O 2002 *Appl. Phys. Lett.* **80** 1204

[22] Vurgaftman I and Meyer J R 2003 *J. Appl. Phys.* **94** 3675